



## Momentum profile analysis in one-neutron knockout from Borromean nuclei

Yu. Aksyutina<sup>a</sup>, T. Aumann<sup>b</sup>, K. Boretzky<sup>a</sup>, M.J.G. Borge<sup>c</sup>, C. Caesar<sup>a</sup>, A. Chatillon<sup>a</sup>, L.V. Chulkov<sup>a,d</sup>, D. Cortina-Gil<sup>a,e</sup>, U. Datta Pramanik<sup>f</sup>, H. Emling<sup>a</sup>, H.O.U. Fynbo<sup>g</sup>, H. Geissel<sup>a</sup>, G. Ickert<sup>a</sup>, H.T. Johansson<sup>h</sup>, B. Jonson<sup>h,\*</sup>, R. Kulesa<sup>i</sup>, C. Langer<sup>a</sup>, T. LeBlais<sup>a</sup>, K. Mahata<sup>a</sup>, G. Münzenberg<sup>a</sup>, T. Nilsson<sup>h</sup>, G. Nyman<sup>h</sup>, R. Palit<sup>j</sup>, S. Paschalis<sup>k</sup>, W. Prokopowicz<sup>a</sup>, R. Reifarth<sup>a,j</sup>, D. Rossi<sup>a</sup>, A. Richter<sup>b,l</sup>, K. Riisager<sup>g</sup>, G. Schrieder<sup>b</sup>, H. Simon<sup>a</sup>, K. Sümmerer<sup>a</sup>, O. Tengblad<sup>c</sup>, H. Weick<sup>a</sup>, M.V. Zhukov<sup>h</sup>

<sup>a</sup> GSI Helmholtzzentrum für Schwerionenforschung GmbH, ExtreMe Matter Institute, EMMI, D-64291 Darmstadt, Germany

<sup>b</sup> Institut für Kernphysik, Technische Universität, D-64289 Darmstadt, Germany

<sup>c</sup> Instituto Estructura de la Materia, CSIC, E-28006 Madrid, Spain

<sup>d</sup> Kurchatov Institute, RU-123182 Moscow, Russia

<sup>e</sup> University of Santiago de Compostela, 15706 Santiago de Compostela, Spain

<sup>f</sup> Saha Institute of Nuclear Physics, 1/AF Bidhannagar, Kolkata 700064, India

<sup>g</sup> Department of Physics and Astronomy, University of Aarhus, DK-8000 Aarhus C, Denmark

<sup>h</sup> Fundamental Fysik, Chalmers Tekniska Högskola, S-412 96 Göteborg, Sweden

<sup>i</sup> Instytut Fizyki, Uniwersytet Jagielloński, PL-30-059 Kraków, Poland

<sup>j</sup> Institut für Kernphysik, Johann-Wolfgang-Goethe-Universität, D-60486 Frankfurt, Germany

<sup>k</sup> Oliver Lodge Laboratory, University of Liverpool, Liverpool L69 7ZE, United Kingdom

<sup>l</sup> ECT\*, Villa Tambosi, I-38100 Villazzano (Trento), Italy

### ARTICLE INFO

#### Article history:

Received 31 August 2012

Received in revised form 12 December 2012

Accepted 12 December 2012

Available online 14 December 2012

Editor: D.F. Geesaman

### ABSTRACT

One-neutron knockout reactions from Borromean nuclei are analyzed using a profile function analysis technique. The profile function, which is derived as the square root of the variance of the measured fragment + neutron momenta as a function of their relative energy, is shown to be very sensitive to the angular momentum of the knocked out neutron. Three cases are studied here:  ${}^7\text{He}$ , where the profile function analysis shows a presence of  $(s_{1/2})^2$  component in the  ${}^8\text{He}$  ground-state wave-function,  ${}^{10}\text{Li}$ , where the presence of a 11(2)%  $d$ -wave contribution to the relative energy spectrum above 1.5 MeV is found and, finally, the presence of a major  $s$  contribution around 0.5 MeV relative energy in the  ${}^{13}\text{Be}$  case and that the observed decay to the  ${}^{12}\text{Be}$   $2^+$  state originates in a  $d$  state in  ${}^{13}\text{Be}$ .

© 2012 Elsevier B.V. Open access under CC BY license.

In the quest for a deeper understanding of the structure of the lightest elements it is important to study the very short-lived nuclei at the edge of particle stability as well as their unbound neighbors in great detail. The swift existence of the unbound isotopes makes them particularly difficult to reach. Due to the availability of energetic beams of very exotic radioactive nuclear species there has been a tremendous development in this area of modern nuclear physics. Exotic nuclei, like  ${}^8\text{He}$ ,  ${}^{11}\text{Li}$  and  ${}^{14}\text{Be}$ , have acted as stepping stones towards the even more exotic nuclides. Verifying the mere existence of the unbound isotopes is a challenge as such. Enlarging the amount of structural information needs different ingenious methods of analysis in deep concord with theory. To seek such experimental observables capable of extracting maximal information from the data has pushed the field forward in a

spectacular way. Examples are the analysis of momentum distributions, relative energy spectra, and energy and angular correlations among the decay products [1]. In this *Letter* we introduce an additional method of analysis, based on a study of the variance of the momenta of the reaction products, which turns out to be particularly sensitive to the angular momentum content. To illustrate the strength of the method we apply it to the three unbound nuclei  ${}^7\text{He}$ ,  ${}^{10}\text{Li}$  and  ${}^{13}\text{Be}$ , produced in neutron-knockout reactions from the Borromean nuclei  ${}^8\text{He}$ ,  ${}^{11}\text{Li}$  and  ${}^{14}\text{Be}$ , respectively. In all three cases we arrive at new spectroscopic information.

From the derived four-momenta of neutrons and fragments, after one-neutron knockout reactions, we first calculate the relative energy between the neutron and the fragment,  $E_{fn}$ , which results in a relative energy spectrum binned in regular energy intervals. The next step is then to calculate the variance of the momentum of the  $f+n$  system,  $p_{f+n}^x = (p_f^x + p_n^x)$ , transverse to the beam direction for the group of events within each energy bin. Note that in the sudden approximation the absolute value  $p_{f+n}^x$  is equal to

\* Corresponding author.

E-mail address: Bjorn.Jonson@chalmers.se (B. Jonson).

the momentum of the knocked out neutron inside the projectile before the collision. The group of events within the energy bin is thus represented by a number (in units of momentum squared) and its square root,  $P(E_{fn})$ , is plotted as a function of  $E_{fn}$ . The spectrum obtained in this way is defined as the profile function,

$$P(E_{fn}) = \sqrt{\langle (p_{f+n}^x)^2 \rangle - \langle p_{f+n}^x \rangle^2}. \quad (1)$$

Such an experimental profile function can then be compared to a theoretical profile function. In this analysis the theoretical variance was calculated using the probability density function from Ref. [2,3], where the parameters are the neutron separation energy in the projectile and a cut-off parameter,  $x_0$ . Collisions at impact parameters smaller than  $x_0$  are assumed to lead to core fragmentation and do not add to the measured reaction channel. The  $l$  dependence of the profile function is very pronounced [2]. It has been shown experimentally that the widths of the longitudinal and transverse momentum distributions are equal to within 10% and does not depend on the radius of target nuclei to a level of 10% [4]. In application to a neutron knockout from Borromean nuclei the shapes of momentum distributions in longitudinal and transverse directions are the same [5].

The data analyzed in this Letter originate from an experiment performed at the ALADIN-LAND setup at GSI, where one-neutron knockout reactions were studied by bombarding a liquid hydrogen target [6] with beams of  ${}^8\text{He}$  ( $E = 240$  MeV/u),  ${}^{11}\text{Li}$  ( $E = 280$  MeV/u) and  ${}^{14}\text{Be}$  ( $E = 304$  MeV/u). The selection of coincidences between one neutron and the corresponding  $A(Z, N - 2)$  fragment gave the one-neutron knockout residues as described in Refs. [7,8]. The fragment momentum resolution was determined by measuring the transverse momentum of the  ${}^8\text{He}$ ,  ${}^{11}\text{Li}$  and  ${}^{14}\text{Be}$  beams. The influence of the uncertainty in  $p_n^x$  on  $p_{f+n}^x$  was checked and found to be negligible. The  $p_{f+n}^x$  resolution functions for  ${}^6\text{He} + n$ ,  ${}^9\text{Li} + n$  and  ${}^{12}\text{Be} + n$  are shown in Fig. 1 (lower panel). The profile functions  $P(E_{fn})$  were corrected for the resolution. The resolution of the relative energy,  $E_{fn}$ , is on the other hand mainly determined by the experimental resolution of neutron momentum and remains therefore the same for the three cases,  ${}^6\text{He} + n$ ,  ${}^9\text{Li} + n$  and  ${}^{12}\text{Be} + n$  studied in this experiment. The resolution function is given as  $\sigma = 0.18E_{fn}^{0.75}$  MeV. The value  $x_0 = 2.2$  fm<sup>1</sup> was obtained from a fit to the  ${}^7\text{He}$  momentum distribution in  $0 < E_{fn} < 1$  MeV energy region where  $3/2^-$  resonance dominates. The corresponding momentum distribution is shown in Fig. 1 (upper panel). The experimental data were also corrected for the cases when two neutrons cross the LAND area but only one of them was detected.

To start with, the knock-out data from  ${}^8\text{He}$  are investigated. The  ${}^6\text{He} + n$  coincidences give access to the unbound  ${}^7\text{He}$  nucleus. This nucleus has been studied in many different experiments using a variety of approaches (see Ref. [9] and references therein). There is a general consensus that its ground state is a  $p_{3/2}$  resonance with configuration  ${}^6\text{He} \otimes (0p_{3/2})$ , where the spectroscopic factor was found to be 0.61 in Ref. [8] and 0.51 in Ref. [9]. Fig. 2 displays the experimental relative energy spectrum and the profile function for  ${}^7\text{He}$ . The solid curve in the lower panel is a fit to the experimental data with a pure  $p_{3/2}$  resonance at 0.39(2) MeV ( $\Gamma = 0.19(3)$  MeV) folded with the experimental resolution [8]. The three curves in the upper panel show the calculated profile functions for pure  $s$ -,  $p$ - and  $d$ -waves of the removed neutron. It is seen that the main part of the experimental profile function reveals the theoretically expected slope. There is, however,

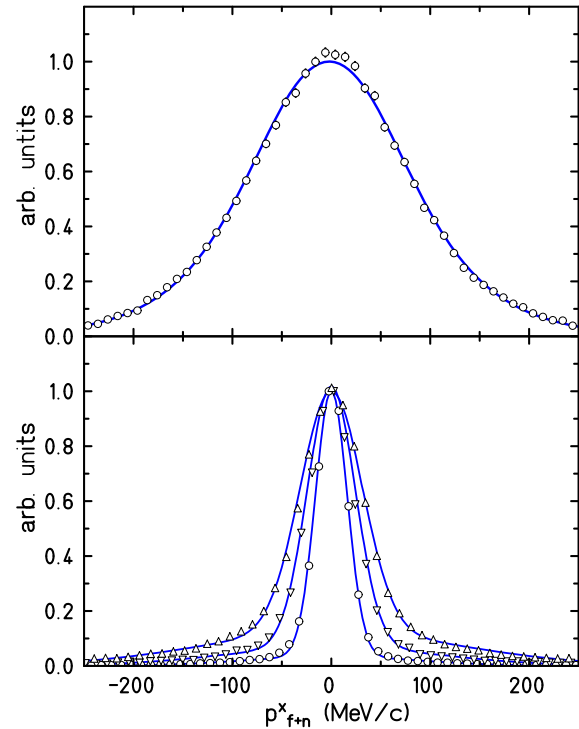
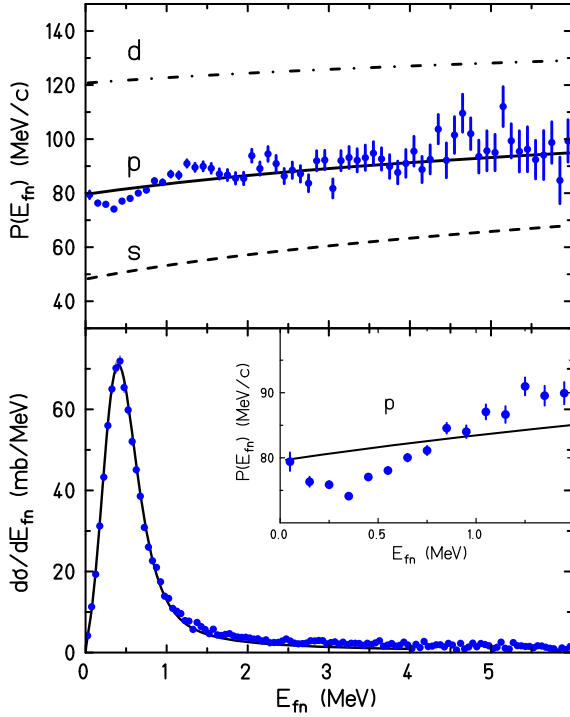


Fig. 1. Upper panel: Distribution of the  ${}^6\text{He} + n$  transverse momentum in fragmentation of  ${}^8\text{He}$  on a liquid hydrogen target obtained in the energy region  $0 < E_{fn} < 1$  MeV. The solid line is a fit by the model described in Refs. [2,3] with  $\ell = 1$  and with  $x_0 = 2.2$  fm. Lower panel: Resolution functions of transverse momentum for  ${}^6\text{He} + n$ , circles,  ${}^9\text{Li} + n$ , inverted triangles, and  ${}^{12}\text{Be} + n$ , triangles.

an interesting small deviation from this main trend in the vicinity of the maximum of the  $3/2^-$  resonance, as illustrated in the inset of Fig. 2. We interpret this deviation as originating from the structure of  ${}^8\text{He}$ . The  ${}^8\text{He}$  projectile is expected to have its main configuration as  ${}^4\text{He} \otimes (0p_{3/2})^4$ . One may also expect that there are components in the wave-function with the two last neutrons in  $(0p_{1/2})^2$ ,  $(1s_{1/2})^2$  or even  $(0d_{5/2})^2$  configurations. The profile function is sensitive to the  $l$  value, which means that deviation below the  $p$  curve represents a contribution from an  $l = 0$  component. Such a component in the ground state of  ${}^8\text{He}$  was predicted in Ref. [10] using a *core + 4n* model with density-dependent contact interaction by solving the five-body Hamiltonian in the Hartree-Fock-Bogoliubov approximation. We may also compare our result with an analysis of  ${}^9\text{He}$  [8], which is a pure  $p_{3/2}$  single-particle state. A deviation from the expected  $p_{3/2}$  shape of the  $E_{fn}$  spectrum at low energy revealed a 12%  $(1s_{1/2})^2$  component in  ${}^6\text{He}$ . In the  ${}^8\text{He}$  case such a distortion of the relative energy spectrum is not easy to observe since the maximum in the  $p_{3/2}$  distribution lies at about 0.4 MeV, close to the maximum of the  $1s_{1/2}$  shape. It is, however, a clear indication of an  $s$ -wave contribution and it is in this case only through the profile function analysis that one may observe such subtleties in the data.

The second well-known unbound system analyzed here is the binary subsystem  ${}^9\text{Li} + n$  after one-neutron knockout from  ${}^{11}\text{Li}$ . This is a slightly more complex case, where the unbound nucleus  ${}^{10}\text{Li}$  is characterized by a virtual  $s$ -state (scattering length  $-22(5)$  fm) at low relative energy together with a  $p$ -wave resonance at 0.57 MeV ( $\Gamma = 0.55$  MeV [7]). The experimental  $E_{fn}$  spectrum is shown in Fig. 3 (lower panel). The corresponding experimental momentum profile function  $P_{exp}(E_{fn})$  together with calculations for different  $l$ -values are plotted in the upper panel. The solid curve in Fig. 3 (upper panel) shows the profile function  $P_{r.e.}(E_{fn})$  calculated by using the weight of  $s$ -component  $\alpha$

<sup>1</sup> This value is kept fixed in the three cases studied here.



**Fig. 2.** Upper panel: Momentum profile for the  ${}^6\text{He} + n$  system after one-neutron knockout from  ${}^8\text{He}$ . The solid line is the calculated  $p$ -wave momentum profile, which is fitted to the experimental data. The  $s$ - and  $d$ -profile functions are also shown as an illustration of the large separation between the different  $l$  components, which makes this type of analysis very sensitive. Lower panel: Relative energy spectrum for  ${}^6\text{He} + n$  [8]. The solid line is the result of an R-matrix fit to the data folded with the experimental resolution [8]. The inset shows the profile function in the low energy region, where the deviation is interpreted as due to knockout from a  $(1s_{1/2})^2$  component in the  ${}^8\text{He}$  ground-state wave-function.

in the  $E_{fn}$  spectrum [7] determined from the fit:  $P_{r.e.}(E_{fn}) = \sqrt{\alpha_s \sigma_s^2 + (1 - \alpha_s) \sigma_p^2}$ , where  $\sigma_s^2$  and  $\sigma_p^2$  are calculated variances for  $l = 0$  and  $l = 1$ , respectively. The profile function  $P_{r.e.}(E_{fn})$  is here given up to 6 MeV and one notes that the fit with only  $s$  and  $p$  components follow the experimental data only up to about 1.5 MeV. In the energy region from 1.5 MeV on one notes an increasing excess all the way up to the top of the spectrum. This excess is interpreted as due to knock-out from  $(d_{5/2})^2$  component in the  ${}^{11}\text{Li}$  ground-state wave-function. The relative weight of  $(d_{5/2})^2$  component in the  $E_{fn}$  spectrum  $\alpha_d$  was obtained by using the relation:  $\alpha_d = (P_{exp}^2 - P_{r.e.}^2) / (\sigma_d^2 - P_{r.e.}^2)$  for  $E_{fn} > 1.5$  MeV. The size of this contribution is 11(2)%, a result which is in agreement with the earlier determined value of 17(5)% obtained in Ref. [11] from an analysis of the transverse momentum distribution. One can also see that the fit to the relative energy spectrum falls below the experimental data at high energies. The knock-out from the  $d$ -wave states populates the narrow states in  ${}^{10}\text{Li}$ , with structure  $[d_{5/2} \otimes (3/2^-)]_{1^-, 2^-, 3^-, 4^-}$ . We can, however, not resolve such states with our experimental resolution but the profile function analysis adds the information that the  $d$ -wave strength is distributed in the energy region between 1.5 to 6 MeV.

While the high-statistics data for  ${}^7\text{He}$  and  ${}^{10}\text{Li}$  has been discussed earlier [7,8] we present here, as our third case, for the first time the new data for  ${}^{13}\text{Be}$ . Also here the resolution and statistics are superior to that of our earlier paper [11]. A major problem in the interpretation of  ${}^{13}\text{Be}$  originates in the complex nuclear structure of the neutron-rich beryllium isotopes. It was enunciated already in 1976 that several observed properties of the  $T = 2$ ,  $I^\pi = 0^+$  states of  $A = 12$  nuclei favor a model of the  ${}^{12}\text{Be}$  ground-

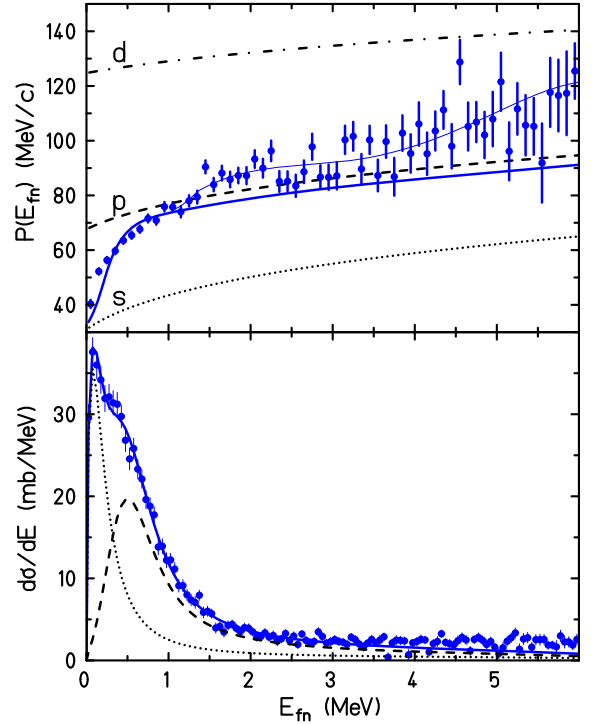


**Fig. 3.** Upper panel: Momentum profile of the  ${}^9\text{Li} + n$  system after one-neutron knockout from  ${}^{11}\text{Li}$ . The calculated  $s$ - (dashed),  $p$ - (dotted) and  $d$ -wave (dash-dotted) momentum profiles are shown together with a solid line determined from the  $s$ -to- $p$  ratio derived from the data in the lower panel. The thin-solid line is a smooth line through experimental points. Lower panel: Relative energy spectrum for  ${}^9\text{Li} + n$  [7]. The different contributions from a R-matrix fit to the data, folded with the experimental resolution, are shown as dotted (virtual  $s$ -state) and dashed ( $p$ -wave resonance) lines with the solid line as their sum.

state wave-function being made up of only small components that belong to the lowest shell-model configurations, while instead  $s$ -,  $p$ - and  $d$ -shells are populated with almost equal weights [12,13],

$${}^{12}\text{Be}(g.s.) = \alpha [{}^{10}\text{Be} \otimes (1s_{1/2})^2] + \beta [{}^{10}\text{Be} \otimes (0p_{1/2})^2] + \gamma [{}^{10}\text{Be} \otimes (0d_{5/2})^2]. \quad (2)$$

Here,  ${}^{10}\text{Be}$  forms an inert core with a closed  $0p_{3/2}$  neutron shell. This conjecture has actually been confirmed in a series of recent experiments [14–18]. In Ref. [14] it was found that  $N = 8$  is not a good closed shell for  ${}^{12}\text{Be}$  since it contains a major  $(s^2 - d^2)$  intruder configuration. This breakdown of the  $N = 8$  shell closure is also expected theoretically [13,19–24]. This means that the structure of  ${}^{12}\text{Be}$  essentially is of few-body character and that a description of  ${}^{13}\text{Be}$  with a  ${}^{12}\text{Be}$  core having a closed  $p_{1/2}$  shell is not a good approximation. The open decay channels from  ${}^{13}\text{Be}$  to excited states in  ${}^{12}\text{Be}$  makes the situation even more complicated [11,25]. If the remaining fragment, after neutron knockout from a Borromean nucleus, is left in an excited, gamma-decaying state, the corresponding peak in the  $E_{fn}$  spectrum will be shifted towards low energies by the excitation energy of the fragment.

The difficulty in the interpretation of  ${}^{13}\text{Be}$  data is illustrated by the three relatively recently published data sets, all with different interpretation of the momentum content around 0.5 MeV in the excitation spectrum. From data obtained at GANIL [26] it is interpreted as a Breit-Wigner  $l = 0$  resonance; from the one-neutron knockout data from  ${}^{14}\text{Be}$ , measured earlier at GSI, as a dominating virtual  $s$ -state [11]; and, finally, from data obtained at RIKEN [25] it is interpreted as an  $l = 1$  resonance together with a small contribution from a virtual  $s$  state.

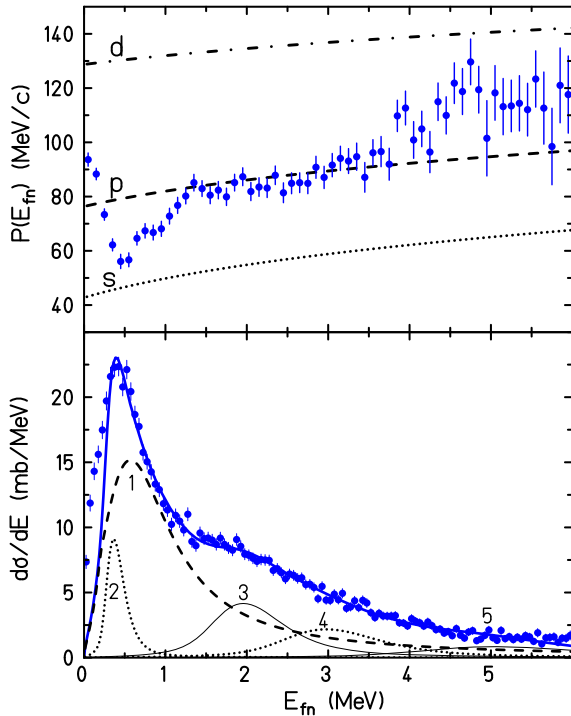


**Fig. 4.** Upper panel: Momentum profile of the  $^{12}\text{Be} + n$  system after one-neutron knockout from  $^{14}\text{Be}$  when impinging on a hydrogen target. The results of model calculations are shown as a dashed line ( $s$ -wave), a dotted line ( $p$ -wave) and a dashed-dotted line ( $d$ -wave). Lower panel: Relative energy spectrum for  $^{12}\text{Be} + n$  and its resonance-state decomposition based on the interpretation given in Ref. [11]: (1)  $-1/2^+$ , (2 & 4)  $-1/2^-$ , (3 & 5)  $-5/2^+$ .

In order to shed more light on this discrepancy and to overcome it, we here apply the profile function analysis to our new data, and limit in this *Letter* the discussion to relative energy up to 1 MeV in  $^{12}\text{Be} + n$ . Due to the complexity of the  $^{13}\text{Be}$  case we give here only two distinct results in this *Letter* where the profile function gives additional insight. A complete analysis of  $^{13}\text{Be}$ , with these results in mind, will be the subject of a forthcoming paper.

The relative energy spectrum  $^{12}\text{Be} - n$  is shown in the lower panel of Fig. 4. As a starting point for the present discussion we perform an R-matrix fit to our new data under the same assumption of the relative  $s$ -,  $p$ - and  $d$ -contributions as in Fig. 10 of Ref. [11]. With the improved resolution one notes immediately that the low energy part of the relative energy spectrum cannot be described with these assumptions alone. This observation combined with the profile function indicates that the low energy strength must originate in a  $d$ -wave contribution. This may be understood as follows: There is one state in  $^{13}\text{Be}$  [27–30] at an energy of about 2 MeV, which is expected to be  $5/2^+$  state. This state would then have one component with the structure  $[^{12}\text{Be}(2^+) \otimes (1s_{1/2})]_{5/2^+}$  [31,32], which can decay via neutron emission to the  $2^+$  state in  $^{12}\text{Be}$ . The  $^{12}\text{Be}(2^+)$  state is then de-excited via  $\gamma$ -emission to the ground state of  $^{12}\text{Be}$ . Kondo et al. [25], observed indeed neutron-gamma coincidences at low  $E_{fn}$ , and the profile function adds the information that origin of the increase of the profile function above the  $p$ -wave curve is due to its origin in a  $5/2^+$  resonance in  $^{13}\text{Be}$ . In the interval from the beginning of the relative energy to 0.5 MeV one observes a rapid decrease of the experimental profile function, far below values expected for a  $p$ -wave. The pure fact that the profile function falls down close to the  $s$  curve is an indication of a large  $s$  contribution. In the region from 300 keV to 1 MeV assuming only  $s$ - and  $p$ -contributions, one may estimate in the order of 60%  $s$ -wave

contribution. The presence of an additional  $d$  configuration in this region would result in an even larger value. This is rather in favor of the interpretation given in Refs. [26] and [11]. A  $1/2^+$  state at low energy in  $^{13}\text{Be}$  should have the configuration

$$^{13}\text{Be}(1/2^+) = \zeta [^{10}\text{Be} \otimes (0p_{1/2})^2 \otimes (1s_{1/2})] + \eta [^{10}\text{Be} \otimes (0d_{5/2})^2 \otimes (1s_{1/2})]. \quad (3)$$

The maximum at 0.5 MeV in the relative energy spectra from Refs. [11,25] and from data analyzed here is more narrow than the ones in Ref. [26] where states of  $^{13}\text{Be}$  have been populated by proton knockout from  $^{14}\text{B}$ . The large momentum transfer to the core in a knockout of a tightly-bound proton can be the reason. Such an effect has been observed in [6] for the  $^8\text{He} + n$  system in proton knockout reactions from  $^{11}\text{Li}$ .

The conclusion, based on the information from the momentum profile analysis, is that the main peak in the relative energy spectrum  $^{12}\text{Be} + n$ , is to a major part associated with an  $s$  state.

In summary we have used an experimental observable, the momentum profile function of the remaining fragment + neutron system after one-neutron knockout from a Borromean nucleus, to study details in the angular momentum content in the binary residue. This method have the same limitations as those for momentum distributions: high beam energy is needed in order adopt impulse approximation and a hydrogen target is preferable. We have observed the following new results:

- (i) The  $^7\text{He}$  data reveals the presence of an  $(s_{1/2})^2$  component in the  $^8\text{He}$  ground-state wave-function.
- (ii) The  $^{10}\text{Li}$  data reveals an 11(2)%  $(d_{5/2})^2$  component in the  $^{11}\text{Li}$  ground-state wave-function. The  $d$ -wave strength is found to contribute to the  $^{10}\text{Li}$  relative energy spectrum in the energy region above 1.5 MeV.
- (iii) We confirm an  $s$  wave neutron decay from a  $5/2^+$  state in  $^{13}\text{Be}$  to the 2.1 MeV  $2^+$  state in  $^{12}\text{Be}$ . It is shown that the maximum in the  $^{13}\text{Be}$  relative energy spectrum has a strong contribution from an  $s$  state.

## Acknowledgements

The authors are indebted to A. Bonaccorso and A. Heinz for numerous discussions.

This work is partly supported by the Helmholtz International Center for FAIR within the framework of the LOEWE program launched by the State of Hesse. Financial support from the Swedish Research Council and the Spanish Ministry through the research grant FPA2009-07387 is also acknowledged.

## References

- [1] B. Jonson, Phys. Rep. 389 (2004) 1.
- [2] P.G. Hansen, Phys. Rev. Lett. 77 (1996) 1016.
- [3] D. Bazin, et al., Phys. Rev. 57 (1998) 2156.
- [4] D.E. Greiner, et al., Phys. Rev. Lett. 35 (1975) 152.
- [5] T. Aumann, et al., Nucl. Phys. A 640 (1998) 24.
- [6] H.T. Johansson, et al., Nucl. Phys. A 842 (2010) 15.
- [7] Yu. Aksyutina, et al., Phys. Lett. B 666 (2008) 430.
- [8] Yu. Aksyutina, et al., Phys. Lett. B 679 (2009) 191.
- [9] Z.X. Cao, et al., Phys. Lett. B 707 (2012) 46.
- [10] K. Hagino, N. Takahashi, H. Sagawa, Phys. Rev. C 77 (2008) 054317.
- [11] H. Simon, et al., Nucl. Phys. A 791 (2007) 267.
- [12] F.C. Barker, J. Phys. G: Nucl. Part. Phys. 2 (1976) L45.
- [13] F.C. Barker, J. Phys. G: Nucl. Part. Phys. 36 (2009) 038001.
- [14] A. Navin, et al., Phys. Rev. Lett. 85 (2000) 266.
- [15] S.D. Pain, et al., Eur. Phys. J. A 25 (2005) 349.
- [16] H. Iwasaki, et al., Phys. Lett. B 481 (2000) 7.
- [17] S. Shimoura, et al., Phys. Lett. B 654 (2007) 87.
- [18] R. Kanungo, et al., Phys. Lett. B 682 (2010) 391.

- [19] T. Suzuki, T. Otsuka, *Phys. Rev. C* 56 (1997) 847.
- [20] M. Labiche, F.M. Marques, O. Sorlin, N. VinhMau, *Phys. Rev. C* 60 (1999) 027303.
- [21] H.T. Fortune, R. Sherr, *Phys. Rev. C* 74 (2006) 024301.
- [22] G. Blanchon, et al., *Nucl. Phys. A* 784 (2007) 49.
- [23] H.T. Fortune, R. Sherr, *J. Phys. G: Nucl. Part. Phys.* 36 (2009) 038002.
- [24] G. Blanchon, N.V. Mau, A. Bonaccorso, M. Dupuis, N. Pillet, *Phys. Rev. C* 82 (2010) 034313.
- [25] Y. Kondo, et al., *Phys. Lett. B* 690 (2010) 245.
- [26] J.L. Lecouey, *Few-Body Systems* 34 (2004) 21.
- [27] D.V. Aleksandrov, et al., *Yad. Fiz.* 37 (1983) 797;  
D.V. Aleksandrov, et al., *Sov. J. Nucl. Phys.* 37 (1983) 474.
- [28] A.N. Ostrovski, et al., *Z. Phys. A* 343 (1992) 489.
- [29] A.V. Belozarov, et al., *Nucl. Phys. A* 636 (1998) 419.
- [30] A.A. Korshennikov, et al., *Phys. Lett. B* 343 (1995) 53.
- [31] H.T. Fortune, R. Sherr, *Phys. Rev. C* 82 (2010) 064302.
- [32] T. Tarutina, I.J. Thompson, J.A. Tostevin, *Nucl. Phys. A* 733 (2004) 53.